COMPUTER ANALYSIS OF CONSECUTIVE PHOTOCHEMICAL REACTIONS

BRIAN S. ERLER and DAVID R. TYLER
Department of Chemistry, Columbia University, New York, NY 10027 (U.S.A.)
(Received September 22, 1981)

Summary

A computer program was written to analyze consecutive photochemical reactions of the type

$$A \underset{h\nu}{\overset{h\nu}{\rightleftharpoons}} B \xrightarrow{h\nu} C$$

If the experimental values for the concentrations of A, B and C *versus* time are known, then the program can calculate the quantum yields of the partial reactions. Conversely, if the quantum yields of the partial reactions are known, then the program will calculate the concentrations of A, B and C after a given irradiation time. The program will also calculate the time required to obtain the maximum amount of B. To test the computational validity of the program the photosubstitution of $W(CO)_6$ by pyridine was studied: $W(CO)_6 \rightarrow W(CO)_5py \rightarrow$ *cis*-$W(CO)_4(py)_2$. The concentrations of the tungsten carbonyl species were monitored by IR spectroscopy and compared with the calculated concentrations; good agreement was obtained. Applications of the program to synthetic and mechanistic studies are discussed.

---

1. Introduction

Consecutive reactions are common in the photochemistry of organometallic complexes. An example is shown below ($Cp \equiv \eta^5$-C_5H_5) [1]:

$$2CpW(CO)_3CH_3 \xrightarrow[CCl_4]{h\nu} Cp_2W_2(CO)_6 \xrightarrow[CCl_4]{h\nu} 2CpW(CO)_3Cl \qquad (1)$$

Quantitative studies of consecutive reactions are possible if the intermediate product is stable and isolable. In eqn. (1), for example, the species $Cp_2W_2(CO)_6$ is stable and so it is not difficult to obtain the quantum yield for each partial photoreaction comprising eqn. (1). In many cases, however, the intermediate product is not stable or is not isolable in pure form; in these cases it is much more difficult to obtain the partial reaction quantum yields. In our studies we frequently encounter consecutive photochemical reactions

0047-2670/82/0000-0000/$02.75

of the latter type, *i.e.* we spectroscopically observe the formation of a non-isolable intermediate product and then the intermediate product photolyzes to give the final product. Because a knowledge of the partial reaction quantum yields would greatly aid our mechanistic interpretations of these reactions, we decided to design a computer program that would let us extract the quantum yields of the partial reactions from our spectroscopic data on the overall reaction. Our program is applicable to reaction schemes described by

$$aA \underset{h\nu}{\overset{h\nu}{\rightleftharpoons}} bB \xrightarrow{h\nu} cC \tag{2}$$

where a, b and c are stoichiometric coefficients. In this paper we describe our program and its various applications.

2. Experimental details

2.1. Computer program

The input variables for the FORTRAN computer program are the extinction coefficients for A, B and C (if B is a non-isolable intermediate then its extinction coefficient is generally an estimate), the light intensity, the initial concentration of A and the estimated quantum yields for the partial reactions in eqn. (2). Using these input values, the program calculates the concentration *versus* time curves of each of the species A, B and C. The quantum yields giving the best fit to the experimental concentration *versus* time curves are taken as the desired values. The program will also (1) calculate the time t_{max} when the concentration of B in eqn. (2) is at a maximum, (2) calculate the concentrations of A and C at t_{max} and (3) calculate the composition of the reaction mixture at a specified time. (The computer program is available from the authors on request.)

The concentration of species B in eqn. (2) formed during time Δt is given by

$$[B] = \Phi_1 I \frac{b}{a} \frac{\epsilon_A[A]}{\epsilon_A[A] + \epsilon_B[B] + \epsilon_C[C]} V^{-1} F \Delta t \tag{3}$$

where Φ_1 is the quantum yield for the reaction A → B, I is the intensity of the irradiating light in einsteins per minute, a and b are the stoichiometric coefficients of A and B, ϵ_A, ϵ_B and ϵ_C are the molar extinction coefficients of A, B and C, V is the volume of the reaction system in liters and F is a correction factor for the light not absorbed by the species in solution. The concentration of A formed from the back reaction of B in eqn. (2) during time Δt is

$$[A] = \phi_{1B} I \frac{aR_b}{b} \frac{\epsilon_B[B]}{\epsilon_A[A] + \epsilon_B[B] + \epsilon_C[C]} V^{-1} F \Delta t \tag{4}$$

where ϕ_{1B} is the quantum yield of the reaction B → A, $R_b = \phi_{1B}/(\phi_{1B} + \phi_2)$

and ϕ_2 is the quantum yield for the reaction B → C. Finally, the concentration of C formed from B in eqn. (2) is

$$[C] = \phi_2 I \frac{cR_f}{b} \frac{\epsilon_C[C]}{\epsilon_A[A] + \epsilon_B[B] + \epsilon_C[C]} V^{-1} F \Delta t \quad (5)$$

where $R_f = 1 - R_b$.

The factor F is given by the expression

$$F = 1 - 10^{-(\epsilon_A[A]L + \epsilon_B[B]L + \epsilon_C[C]L)}$$

where L is the path length of the reaction cell in centimeters.

The program integrates the concentration curves of the species in solution over time to obtain the composition when the maximum concentration of B is attained. The integration is performed iteratively over small user-defined time intervals using the trapezoidal approximation. The time interval Δt is generally chosen to be of the order of 0.001 min.

The DO loop in the program which performs the iterative integration calculates the molar concentrations of A, B and C formed during a time interval from their respective reactions aA → bB, bB → aA and bB → cC. The total concentrations of A, B and C which were present at the end of the previous time interval are used. The concentrations of A, B and C which appear at the end of the present time interval are added to the A, B and C concentrations from the previous time interval to give a new set of total A, B and C concentrations. At this point the three total concentrations are studied to determine whether the concentration of B has attained its maximum. If requested, the program will store these three concentrations and the time of their appearance in data files which can later be retrieved to create plots of concentration *versus* time using an appropriate plotting program. The plotting program used in this study was compatible with a Versaplot plotting system run on the Digital VAX 11/780 computer.

2.2. Photosubstitution of W(CO)$_6$ by pyridine

The photosubstitution of $W(CO)_6$ by pyridine (py)

$$W(CO)_6 + py \xrightarrow{366\ nm} W(CO)_5py + CO \quad (6)$$

$$W(CO)_5py + py \xrightarrow{366\ nm} cis\text{-}W(CO)_4(py)_2 + CO \quad (7)$$

was used to test the computational validity of our computer program. This reaction sequence was chosen because it has been thoroughly studied by Strohmeier and Von Hobe [2] and Wrighton *et al.* [3]; the quantum yield for each reaction is known and the extinction coefficients for each species at 366 nm are also reported [4]. The input values used in our program to describe reactions (6) and (7) are found in Table 1.

$W(CO)_6$ (1.0×10^{-2} M) was reacted with pyridine (0.5 M) in chloroform solution in a CaF_2 IR cell of 0.010 cm path length so that the reaction could be conveniently monitored by IR spectroscopy. (Chloroform was used

TABLE 1

Input values for the computer analysis of the photoreaction (366 nm) of $W(CO)_6$ (1.0×10^{-2} M) with pyridine (0.5 M)

Variable	*Value*	*Reference*
Φ_1	1.0	[2][a]
Φ_{1B}	0.0	
Φ_2	0.06	[3]
I (einstein min^{-1})	7×10^{-7}	
ϵ_A (M^{-1} cm^{-1})	400	[7]
ϵ_B (M^{-1} cm^{-1})	6500	[3]
ϵ_C (M^{-1} cm^{-1})	7900	[3]
Cell path length[b] (cm)	0.010	
Initial concentration of $W(CO)_6$ (M)	1.0×10^{-2}	
Cell volume (l)	2.5×10^{-5}	

[a] There is some evidence that the quantum yields for photosubstitution of the $M(CO)_6$ complexes (M ≡ Cr, Mo, W) are less than 1.0 [5, 6]. We used the value of 1.0 in our calculations because this value gave the best fit of the experimental data to the calculated data.

[b] The IR cell path length was measured by the interference fringe method [8].

as the solvent for the photoreaction because *cis*-$W(CO)_4(py)_2$ is more soluble in this solvent than in the previously used reaction solvents tetrahydrofuran [2], benzene [2] and iso-octane [3].) A Perkin–Elmer 621 instrument was used to monitor the reaction. The reaction solution was thoroughly degassed by a nitrogen purge prior to its introduction (by syringe) into the IR cell. The solution was irradiated with a 200 W high pressure mercury arc using a Corning CS 7-83 filter to isolate the 366 nm radiation. The concentration of $W(CO)_6$ was monitored by following the disappearance of the band at 1977 cm^{-1} [9]; the concentrations of $W(CO)_5py$ and *cis*-$W(CO)_4(py)_2$ were monitored by their peaks at 1930 and 1887 cm^{-1} respectively [3]. Tungsten hexacarbonyl was obtained from Strem. The pyridine (Aldrich) and the chloroform were dried and distilled by standard methods before use [10]. Light intensities were measured by ferrioxalate actinometry [11].

3. Results and discussion

3.1. The $W(CO)_6$–pyridine system

The results obtained from the 366 nm irradiation of $W(CO)_6$ in chloroform containing 0.5 M pyridine in an IR cell of 0.010 cm path length are summarized in Table 2. The data are shown graphically in Fig. 1. The full curves in Fig. 1 are the calculated curves obtained from the computer program using the input values in Table 1. The calculation predicts that the maximum concentration of $W(CO)_5py$ occurs at 5.4 min. Experimentally, the maximum concentration of $W(CO)_5py$ was reached at 5.3 min. The

TABLE 2

Experimentally determined concentrations of $W(CO)_6$, $W(CO)_5py$ and *cis*-$W(CO)_4(py)_2$ obtained in the 366 nm irradiation of $W(CO)_6$ with pyridine in chloroform solution

Time (min)	$[W(CO)_6]$ ($\times 10^{-2}$ mol l^{-1})	$[W(CO)_5py]$ ($\times 10^{-2}$ mol l^{-1})	[*cis*-$W(CO)_4(py)_2$] ($\times 10^{-2}$ mol l^{-1})
0.00	1.00	0.00	0.000
0.08	0.96	0.038	0.005
0.17	0.93	0.051	0.015
0.33	0.91	0.085	0.026
0.50	0.88	0.11	0.037
0.67	0.84	0.14	0.047
0.92	0.79	0.17	0.063
1.42	0.72	0.23	0.085
1.92	0.64	0.26	0.11
2.42	0.58	0.29	0.13
2.92	0.51	0.31	0.15
3.42	0.47	0.32	0.17
4.17	0.40	0.34	0.19
4.92	0.36	0.36	0.22
5.67	0.32	0.36	0.24
6.17	0.29	0.35	0.25
6.67	0.28	0.35	0.27
7.42	0.25	0.34	0.28
8.17	0.23	0.34	0.29
8.92	0.21	0.33	0.30
9.67	0.19	0.32	0.31
10.42	0.18	0.32	0.32
11.17	0.16	0.31	0.33
11.92	0.15	0.31	0.33

calculated and experimental curves are in close agreement for $W(CO)_6$ and $W(CO)_5py$. For the case of *cis*-$W(CO)_4(py)_2$, experiment shows excessive *cis*-$W(CO)_4(py)_2$ at short irradiation times and too little *cis*-$W(CO)_4(py)_2$ at long irradiation times when compared with the calculated curve. These discrepancies result from the following errors. At short irradiation times (0 - 3 min) it was difficult to determine the absorbance of the 1887 cm^{-1} peak of *cis*-$W(CO)_4(py)_2$ because this peak was only a shoulder on the much more intense $W(CO)_5py$ peak at 1930 cm^{-1}. No attempt was made to subtract the $W(CO)_5py$ absorbance from the experimentally obtained value at 1887 cm^{-1}. Thus, the high experimental values for *cis*-$W(CO)_4(py)_2$ concentration at short irradiation times reflect absorbance readings uncorrected for the $W(CO)_5py$ absorbance. At longer irradiation times (longer than 3 min) this problem no longer presented difficulties because the $W(CO)_5py$ peak at 1930 cm^{-1} was less intense and the *cis*-$W(CO)_4(py)_2$ band at 1887 cm^{-1} was a clearly defined peak. The low concentrations of *cis*-$W(CO)_4(py)_2$ at long irradiation times may be attributable to the photochemical decomposition of *cis*-$W(CO)_4(py)_2$. Control experiments showed that the complex

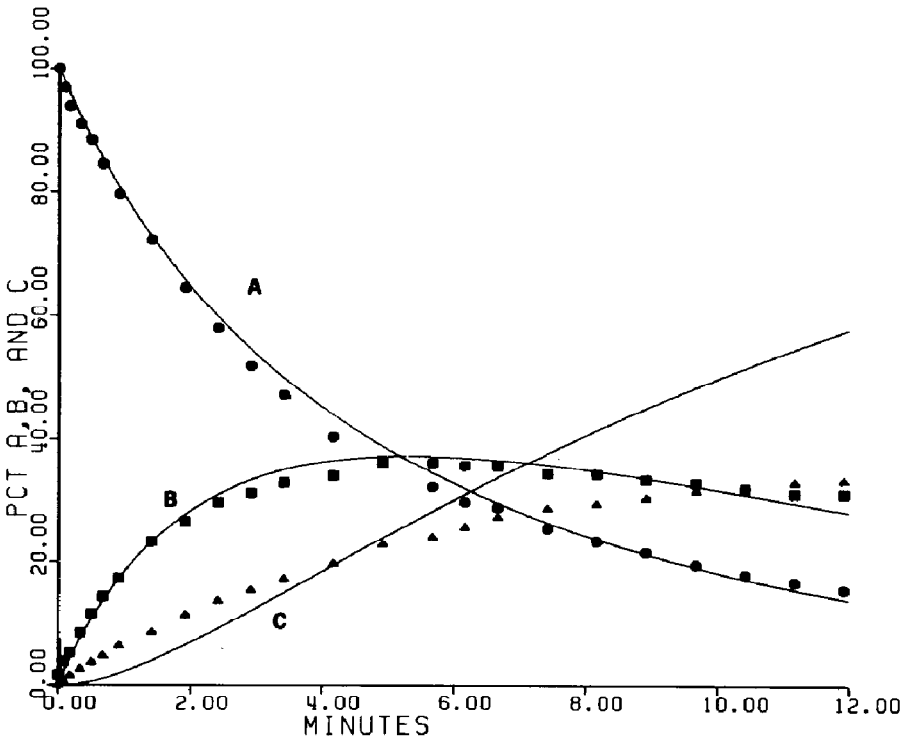

Fig. 1. The calculated and experimental concentration *vs.* time curves for the photochemical reaction (366 nm) of $W(CO)_6$ with pyridine in chloroform under the reaction conditions given in Table 1: curve A, $W(CO)_6$; curve B, $W(CO)_5py$; curve C, *cis*-$W(CO)_4(py)_2$; ——, calculated values; ●, ■, ▲, experimentally determined concentrations.

reacts slowly under the reaction conditions (λ = 366 nm, 0.5 M pyridine in chloroform) to give an unidentified product.

3.2. Anthraquinone in alkaline methanol

Mauser *et al.* [12] have reported the experimental concentration *versus* time curves for the photoreaction of anthraquinone in alkaline methanol:

$$\text{anthraquinone dianion} \xrightarrow{313\ \text{nm}} \text{anthraquinone radical anion}$$

$$\xrightarrow{313\ \text{nm}} \text{anthrahydroquinone dianion} \qquad (8)$$

Their results for this system can also be used to check that our program is functioning properly. The curves in Fig. 2 were generated by our program using the input values reported by Mauser *et al.* (Table 3). A comparison of Fig. 2 with the analogous diagram in the paper by Mauser *et al.* (ref. 12, Fig. 6) shows that the two sets of curves are essentially identical.

The excellent agreement between the experimental and calculated concentration *versus* time curves for the $W(CO)_6$–pyridine and anthraquinone systems shows that our computer program is accurate and that it

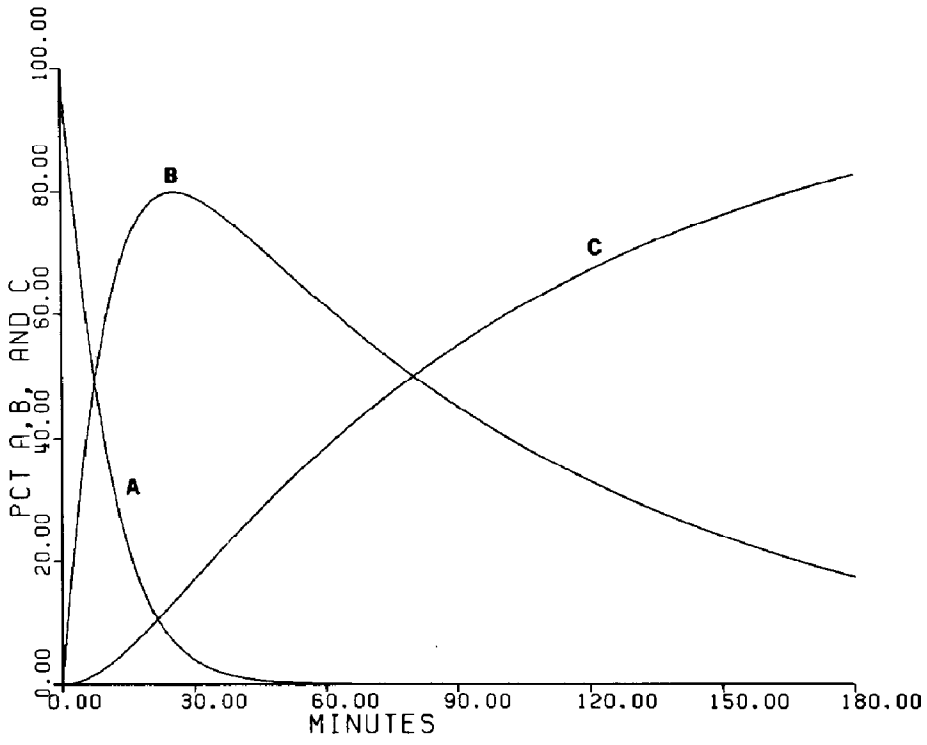

Fig. 2. The calculated concentration *vs.* time curves for the photochemical reaction (313 nm) of anthraquinone in alkaline methanol under the reaction conditions given in Table 3: curve A, anthraquinone; curve B, anthraquinone radical anion; curve C, anthrahydroquinone dianion.

TABLE 3

Input values for the computer analysis of the photoreaction (313 nm) of anthraquinone in alkaline methanol

Variable	*Value*	*Reference*
Φ_1	0.67	[12]
Φ_{1B}	0.0	[12]
Φ_2	0.16	[12]
I[a] (einstein min^{-1})	7.2×10^{-8}	
ϵ_A (M^{-1} cm^{-1})	3930	[12]
ϵ_B (M^{-1} cm^{-1})	1370	[12]
ϵ_C (M^{-1} cm^{-1})	720	[12]
Cell path length[a] (cm)	1.0	
Initial concentration of anthraquinone (M)	1.33×10^{-4}	[12]
Cell volume[a] (l)	3×10^{-3}	

[a] The cell geometry was not reported in ref. 12. A standard 1 cm path length cuvette was therefore assumed. The solution volume was 3 ml. With these assumptions, the reported radiation flux can be converted to an intensity with units of einsteins per minute.

can be applied with confidence to the determination of quantum yields in other consecutive reactions.

3.3. Application to the disproportionation of $Mn_2(CO)_{10}$ in acetonitrile

The application of our program to finding the quantum yields of partial reactions is illustrated by the reaction of $Mn_2(CO)_{10}$ in acetonitrile. When $Mn_2(CO)_{10}$ is irradiated (366 nm) in neat acetonitrile the following reactions occur [13]:

$$Mn_2(CO)_{10} \xrightarrow[CH_3CN]{366\ nm} Mn_2(CO)_9(CH_3CN) \xrightarrow[CH_3CN]{366\ nm} Mn(CO)_3(CH_3CN)_3^+ + Mn(CO)_5^- \quad (9)$$

$Mn_2(CO)_9(CH_3CN)$ is a known species but it was not possible for us to synthesize this material in the exceptionally pure state required for the quantum yield measurement of the reaction

$$Mn_2(CO)_9(CH_3CN) \xrightarrow[CH_3CN]{366\ nm} Mn(CO)_3(CH_3CN)_3^+ + Mn(CO)_5^- \quad (10)$$

Thus, measurement of the partial reaction quantum yields in eqn. (9) is difficult using the conventional method of studying each partial reaction separately.

However, consecutive reactions like those in eqn. (9) are ideally suited for analysis by our program. The only uncertainty in the input data is the extinction coefficient of $Mn_2(CO)_9(CH_3CN)$ at 366 nm; we used a value of 10 000 M^{-1} cm^{-1} by comparison with the extinction coefficient (8900 M^{-1} cm^{-1}) of $Mn_2(CO)_{10}$. This value is reasonable because the replacement of CO by CH_3CN is not expected to alter drastically the electronic structure of $Mn_2(CO)_{10}$ [14]. Using the input data in Table 4, the calculated concentration *versus* time curves in Fig. 3 were generated. The experimental concentrations are shown as points in Fig. 3. A good fit of the calculated to the experimental data is obtained and we conclude that the partial reaction quantum yields are $\phi_1 = 0.43$, $\phi_{1B} = 0.07$ and $\phi_2 = 0.40$.

TABLE 4

Input values for the computer analysis of the photoreaction (366 nm) of $Mn_2(CO)_{10}$ in acetonitrile

Variable	*Value*	*Reference*
ϕ_1	0.43	
ϕ_{1B}	0.07	
ϕ_2	0.40	
I (einstein min^{-1})	3×10^{-6}	
ϵ_A (M^{-1} cm^{-1})	8900	[14]
ϵ_B (M^{-1} cm^{-1})	10000	
ϵ_C (M^{-1} cm^{-1})	400	[13]
Cell path length (cm)	0.10	
Initial concentration of $Mn_2(CO)_{10}$ (M)	6.1×10^{-3}	
Cell volume (l)	2.5×10^{-5}	

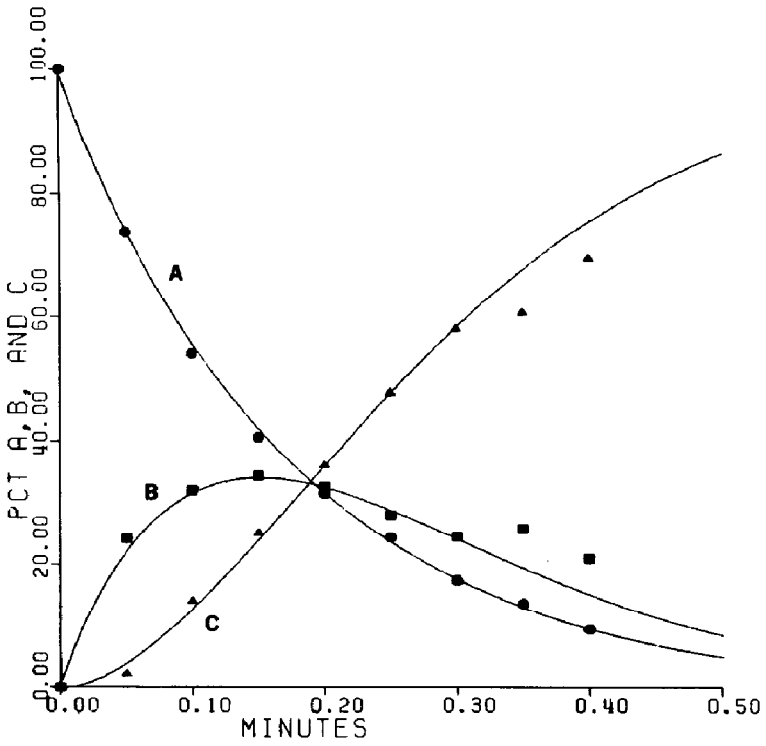

Fig. 3. The calculated and experimental concentration *vs.* time curves for the photochemical reaction (366 nm) of $Mn_2(CO)_{10}$ with acetonitrile under the reaction conditions given in Table 4: curve A, $Mn_2(CO)_{10}$; curve B, $Mn_2(CO)_9(CH_3CN)$; curve C, $Mn(CO)_5^-$; —, calculated values, ●, ■, ▲, experimentally determined concentrations.

3.4. Other applications

Besides being useful for calculating partial reaction quantum yields, the computer program can provide a check on the existence of proposed reaction intermediates. Let us consider the photoreactions in the scheme below

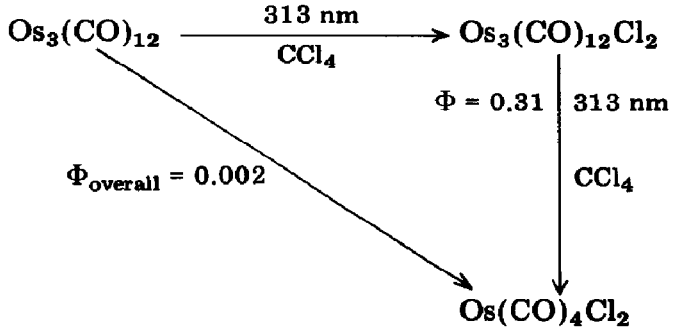

$Os_3(CO)_{12}Cl_2$ has been proposed as an intermediate in the photofragmentation reaction of $Os_3(CO)_{12}$ in carbon tetrachloride giving $Os(CO)_4Cl_2$ [15]. The intermediate $Os_3(CO)_{12}Cl_2$ was not observed spectroscopically, however. It was claimed that the high quantum yield for dis-

appearance of $Os_3(CO)_{12}Cl_2$ in carbon tetrachloride did not allow a spectroscopically detectable concentration of the complex to build up [15]. This proposal can easily be checked with our computer program by using the input variables in Table 5. The calculation reveals that under these conditions the maximum concentration of $Os_3(CO)_{12}Cl_2$ is 5.0×10^{-6} M (Fig. 4). The extinction coefficients for the CO stretching bands of $Os_3(CO)_{12}Cl_2$ have not been reported, but by assuming a reasonable maximum value of 5000 M^{-1} cm^{-1} it can be seen that this concentration is much too low to be detected by IR spectroscopy. A similar calculation using input values suitable for electronic absorption spectroscopy reveals that detection of $Os_3(CO)_{12}Cl_2$ (in the presence of $Os_3(CO)_{12}$ and $Os(CO)_4Cl_2$) by this technique is also not possible.

TABLE 5

Input values for the computer analysis of the photoreaction (313 nm) of $Os_3(CO)_{12}$ with carbon tetrachloride

Variable	*Value*	*Reference*
Φ_1	0.002	[15]
Φ_{1B}	0.0	[15]
Φ_2	0.31	[15]
I (einstein min^{-1})	6×10^{-7}	
ϵ_A (M^{-1} cm^{-1})	7500	[16]
ϵ_B (M^{-1} cm^{-1})	9500	[15]
ϵ_C[a] (M^{-1} cm^{-1})	1000	
Cell path length (cm)	0.10	
Initial concentration of $Os_3(CO)_{12}$ (M)	1.0×10^{-3}	
Cell volume (l)	2.5×10^{-4}	

[a] The electronic spectrum of this complex has not been reported. The extinction coefficient value of 1000 at 313 nm is reasonable for a colorless metal carbonyl complex.

Our computer program is also useful in photochemical syntheses. The situation is frequently encountered in which the product of a photochemical reaction is itself photosensitive at the wavelength used for the irradiation of the reactants. The problem then arises that too long an irradiation time leads to less than the maximum amount of product because of secondary photolysis. Too short an irradiation time, however, also leads to less than optimum yields. For obvious reasons, it is desirable to be able to irradiate the reaction solution for a period of time that gives the maximum amount of product. The optimum irradiation time is easily calculated by our program because the situation described above is really just the consequence of a consecutive photochemical reaction (eqn. (2)). If the quantum yields for the reactions A → B and B → C are known and if the extinction coefficients of A, B and C at the irradiation wavelength are known (or if they can be estimated), then using our program it is possible to calculate the time at which the maximum concentration of B occurs.

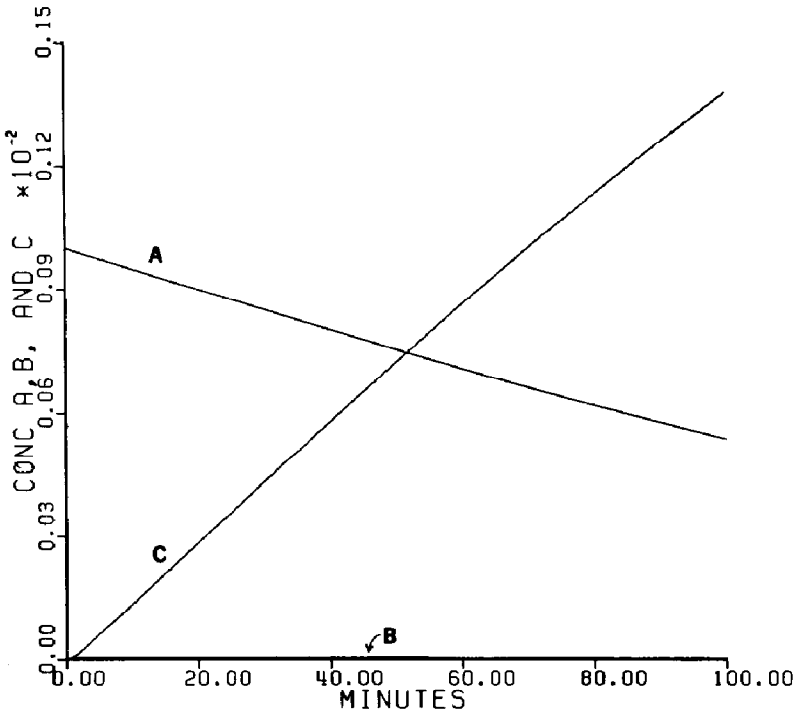

Fig. 4. The calculated concentration *vs.* time curves for the photochemical reaction (313 nm) of $Os_3(CO)_{12}$ in carbon tetrachloride under the reaction conditions given in Table 5: curve A, $Os_3(CO)_{12}$; curve B, $Os_3(CO)_{12}Cl_2$; curve C, $Os(CO)_4Cl_2$.

Acknowledgments

Acknowledgment is made to the Donors of the Petroleum Research Fund, administered by the American Chemical Society, and to the Research Corporation for the support of this research. Mr. Randy Hall is thanked for his expert advice.

References

1 D. R. Tyler, *Inorg. Chem.*, *20* (1981) 2257.
2 W. Strohmeier and D. Von Hobe, *Z. Phys. Chem. (Frankfurt am Main)*, *34* (1962) 393. W. Strohmeier and D. Von Hobe, *Chem. Ber.*, *94* (1961) 2031.
3 M. Wrighton, G. S. Hammond and H. B. Gray, *Mol. Photochem.*, *5* (1973) 179.
4 A. Vogler, in A. W. Adamson and P. D. Fleischauer (eds.), *Concepts of Inorganic Photochemistry*, Wiley, New York, 1975, p. 279.
5 V. Balzani and V. Carassiti, *Photochemistry of Coordination Compounds*, Academic Press, New York, 1970, p. 327.
6 J. Nasielski and A. Colas, *J. Organomet. Chem.*, *101* (1975) 215.
7 N. A. Beach and H. B. Gray, *J. Am. Chem. Soc.*, *90* (1968) 5713.
8 H. H. Willard, L. L. Merritt and J. A. Dean, *Instrumental Methods of Analysis*, Van Nostrand, New York, 5th edn., 1974, p. 165.

9 K. Noack, *Helv. Chim. Acta, 45* (1962) 1847.
10 D. D. Perrin, W. L. F. Armarego and D. R. Perrin, *Purification of Laboratory Chemicals*, Pergamon, Oxford, 1966.
11 J. G. Calvert and J. N. Pitts, *Photochemistry*, Wiley, New York, 1966.
12 H. Mauser, V. Starrock and H.-J. Niemann, *Z. Naturforsch., 27b* (1972) 1354.
13 D. R. Tyler and A. E. Stiegman, unpublished results, 1981.
14 R. A. Levenson and H. B. Gray, *J. Am. Chem. Soc., 97* (1975) 6042.
15 D. R. Tyler, M. Altobelli and H. B. Gray, *J. Am. Chem. Soc., 102* (1980) 3022.
16 D. R. Tyler, R. A. Levenson and H. B. Gray, *J. Am. Chem. Soc., 100* (1978) 7888.